Misfit strain dependence of ferroelectric and piezoelectric properties of clamped (001) epitaxial Pb(Zr0.52,Ti0.48)O3 thin films

Minh D. Nguyen, Matthijn Dekkers, Evert Houwman, Ruud Steenwelle, Xin Wan et al.

Citation: Appl. Phys. Lett. **99**, 252904 (2011); doi: 10.1063/1.3669527
View online: http://dx.doi.org/10.1063/1.3669527
View Table of Contents: http://apl.aip.org/resource/1/APPLAB/v99/i25
Published by the American Institute of Physics.

Misfit strain dependence of ferroelectric and piezoelectric properties of clamped (001) epitaxial $Pb(Zr_{0.52},Ti_{0.48})O_3$ thin films

Minh D. Nguyen,[1,2,3] Matthijn Dekkers,[1,2] Evert Houwman,[1] Ruud Steenwelle,[1] Xin Wan,[1] Andreas Roelofs,[4] Thorsten Schmitz-Kempen,[4] and Guus Rijnders[1,a)]
[1]*MESA+ Institute for Nanotechnology, Faculty of Science and Technology, University of Twente, P.O. Box 217, 7500AE Enschede, The Netherlands*
[2]*SolMateS BV, Drienerlolaan 5 (Bldg. 46), 7522NB Enschede, The Netherlands*
[3]*International Training Institute for Materials Science, Hanoi University of Science and Technology, No. 1 Dai Co Viet road, Hanoi, Vietnam*
[4]*aixACCT Systems GmbH, Talbotstr. 25, 52068 Aachen, Germany*

(Received 27 June 2011; accepted 8 November 2011; published online 22 December 2011)

A study on the effects of the residual strain in $Pb(Zr_{0.52}Ti_{0.48})O_3$ (PZT) thin films on the ferroelectric and piezoelectric properties is presented. Epitaxial (001)-oriented PZT thin film capacitors are sandwiched between $SrRuO_3$ electrodes. The thin film stacks are grown on different substrate-buffer-layer combinations by pulsed laser deposition. Compressive or tensile strain caused by the difference in thermal expansion of the PZT film and substrate influences the ferroelectric and piezoelectric properties. All the PZT stacks show ferroelectric and piezoelectric behavior that is consistent with the theoretical model for strained thin films in the ferroelectric *r*-phase. We conclude that clamped (001) oriented $Pb(Zr_{0.52}Ti_{0.48})O_3$ thin films strained by the substrate always show rotation of the polarization vector. © *2011 American Institute of Physics*. [doi:10.1063/1.3669527]

The properties of ferroelectric thin films can be tuned by changing the temperature or chemical composition. Furthermore, it has also been recognized that the mechanical boundary conditions can influence the ferroelectric and piezoelectric responses significantly.[1] In case of thin films, the difference in crystal lattice parameters and/or the thermal expansion coefficient (TEC) mismatch between the substrate and the clamped thin film upon cooling will result in strain, often referred to as misfit strain (S_M).[2] In epitaxial $Pb(Zr_{1-x}Ti_x)O_3$ (PZT) films much thicker than the critical thickness (>80 nm), the lattice strain is completely relaxed,[3] and the remaining thermal strain is, therefore, either tensile or compressive depending on the choice of substrate. The theoretical dependence of the properties of ferroelectric PZT on this misfit strain has been studied extensively.[4,5] Although some scientific papers report on strain dependency of PZT thin films on various substrates, no experimental data set over a large misfit strain range has been linked to the suggested models. Moreover, most studies on strain dependency are on polycrystalline PZT films. Here, we present experimental ferroelectric and piezoelectric data of *epitaxial* PZT thin films on seven different buffer-layer/substrate combinations in relation to the residual strain.

$SrRuO_3$(100 nm)/PZT(250 nm)/$SrRuO_3$(100 nm) thin film capacitors ($200 \times 200\ \mu m^2$) are fabricated using pulsed laser deposition (PLD) and standard photolithography followed by etching.[6] The used substrates are CeO_2/Yttria stabilized Zirconia (YSZ) buffered Si(001) denoted as S1, $SrTiO_3$ buffered Si(001) – S2,[7] $DyScO_3$(001) – S3, $KTaO_3$(001) – S4 CeO_2 buffered YSZ(001) – S5, MgO(001) – S6, and $SrTiO_3$(001) – S7. The $SrRuO_3$ grows cube-on-cube on the (001) oxide substrates. In the case of S1, S2, and S5, buffer layers were applied to overcome the large lattice mismatch and to control the epitaxial film growth.[6]

Crystallographic properties were investigated by X-ray diffraction (XRD) using a Bruker D8 Discover. The out-of-plane polarization hysteresis loop (*P-E*) measurements were performed using the aixACCT TF2000. The effective longitudinal piezoelectric coefficient ($d_{33,eff}$) was obtained from the piezoelectric loop measured by a double beam laser interferometer (aixACCT DBLI). By using this equipment, the effect of substrate bending is eliminated and the film piezoelectric parameter values are obtained.[8]

Besides the reflections of the substrate and electrodes, the peaks in the XRD spectra in Fig. 1 can be assigned to PZT (00*l*) only. The data indicate that all films are epitaxially grown with (001)-orientation and no second phase is

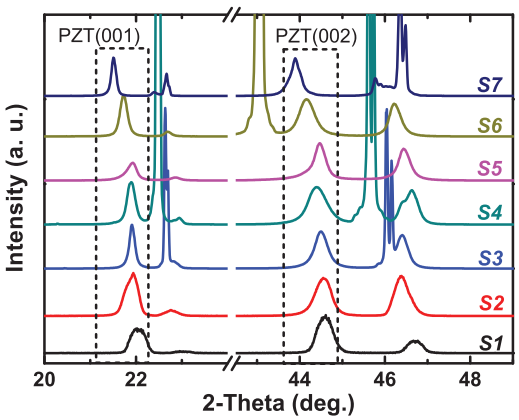

FIG. 1. (Color) XRD patterns of $SrRuO_3$/PZT/$SrRuO_3$ thin films grown on the different substrates S1–S7 showing only PZT (00*l*) thin film orientation.

a)Electronic mail: a.j.h.m.rijnders@utwente.nl.

TABLE I. Measured and calculated properties of the PZT samples on different substrates S1–S7 at room temperature ordered in decreasing misfit strain.

Substrate	Sample	a (Å)	c (Å)	V (Å^3)	S_M (10^{-3})	TEC (10^{-6} K^{-1})	P_3 (μC/cm^2)	P_s (μC/cm^2)	β (°)	ε_{33}	$d_{33,eff}$ (pm/V)	Max $d_{33,eff}$ (pm/V)	Q_{eff} (m^4/C^2)
CeO_2/YSZ/Si	S1	4.108	4.087	68.971	1.71	2.6	20.9	31.4	41.9	378	52.8	72.8	0.038
$SrTiO_3$/Si	S2	4.088	4.080	68.184	0.65	2.6	27.3	34.3	52.6	260	53.5	74.2	0.043
$DyScO_3$	S3	4.062	4.110	67.814	−0.24	8.4	27.3	34.5	52.3	207			
$KTaO_3$	S4	4.089	4.092	68.418	−0.49	6.7	34.8	37.9	66.5	106			
CeO_2/YSZ	S5	4.062	4.092	67.517	−2.45	11.4	35.8	40.4	62.5	184	56.8	74.4	0.049
MgO	S6	4.058	4.106	67.615	−3.91	14.8	46.9	53.0	62.2	183			
$SrTiO_3$	S7	4.061	4.113	67.830	−4.23	11.0	46.5	50.5	67.2	165	72.6	75.2	0.053

observed. From the reciprocal space maps (RSMs) on the four-fold (103) reflections of PZT (not shown), the in- and out-of-plane lattice parameters are obtained (Table I). Furthermore, the (103) RSM appears as one single reflection within the resolution of the diffractometer in all cases. This implies that no mixed *a*- and *c*-domain formation is present in the crystallographic structure of the films. Since the composition is at the morphotropic phase boundary (MPB), the PZT unit-cell is assumed to be (nearly) cubic for an unstrained free standing film. After cooldown the strain induced by the substrate, however, distorts the cubic unit cell and can be calculated as $S_M = (a - a_0)/a_0$, where a is the (measured) in-plane lattice parameter of the PZT thin film.[2,9] a_0 refers to the unstrained cubic in-plane lattice parameter obtained from $a_0 = (a \cdot a \cdot c)^{1/3}$, where c is the (measured) out-of-plane lattice parameter.

Table I shows that S_M (10^{-3}) ranges from about +2 to −4. Indeed, both films on Si are tensile strained because of the lower TEC of this substrate compared to PZT, conversely the strain on oxide crystals is compressive due to the higher TEC. However, S_M is not equal for both Si substrates, indicating that S_M is not proportional to the difference in TEC between film and substrate. The strain relaxation mechanism can be different for the films on each type of substrate, for example by the influence of buffer layers or additional epitaxial strain.[10]

The polarization hysteresis (*P-E*) loops of the PZT capacitors with lowest, intermediate, and highest strain (S1, S5, S7) are shown in Fig. 2(a). Although the PZT thin films have similar orientation, their *P-E* characteristics are substantially different. Whereas large polarization is measured for films with high compressive strain, the values tend to decrease as S_M increases to positive values (tensile strain). The data of the other samples follow this trend but are left out of the graph for clarity. In table I, the out-of-plane polarization P_3 at zero field and the saturated polarization P_s obtained from high field extrapolation are listed for all samples. This trend of decreasing polarization is attributed to the existence of the *r*-phase in which the polarization rotates towards the film plane with increasing misfit strain. To evidence the existence of the *r*-phase, we link the data to the model of Pertsev *et al.*[4] According to this model, PZT films are predicted to be either in the stable ferroelectric *c*-, *r*-, or *aa*-phase, depending on composition and thin film misfit strain. In the *c*-phase, the polarization is along [001] of the pseudo-cube ($P_1 = P_2 = 0$, $P_3 \neq 0$) and in the *aa*-phase along ⟨110⟩ ($P_1 = P_2 \neq 0$, $P_3 = 0$), whereas in the *r*-phase, the polarization rotates in the (1-10) and (−110) planes ($P_1 = P_2 \neq 0$, $P_3 \neq 0$).[2] In Figure 3(a), the calculated stability regions of the different phases as function of S_M versus composition are shown. The *r*-phase is stable in the range $-8 < S_M$ (10^{-3}) $< +8$ for the MPB composition. All of our samples with $x = 0.48$ are well within this regime (Figure 3(a)). Figure 3(b) shows the dependence of the ferro and piezoelectric properties on the misfit strain at zero field. In accordance with the theoretical predictions, the measured P_3 is highest closer to the *c*-phase, and decreases as S_M is more close to the *aa*-phase. Also, the shape of the polarization loops is changed with strain (Fig. 2(a)). The films with high compressive strain show square and well-saturated hysteresis loops, while the films on silicon have more rounded and slanted hysteresis characteristics. This is also evident from the larger difference between P_3 and P_S as S_M increases. In fact, as the *r*-phase is subjected to polarization rotation, this

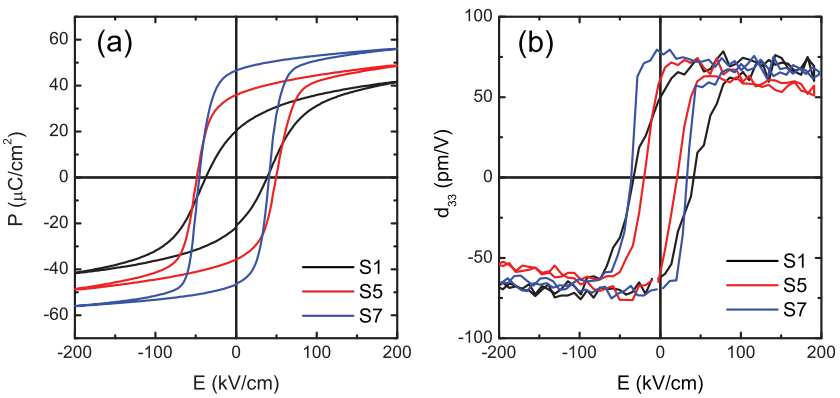

FIG. 2. (Color) (a) P-E loops of the PZT samples S1, S5, and S7, performed at 200 kV/cm amplitude and 1 kHz frequency and (b) d_{33}-E loops of the same PZT samples, measured at AC-voltage of 200 mV and 1 kHz frequency. The base signal is 200 kV/cm at 0.2 Hz and the output signal is averaged over 100 cycles.

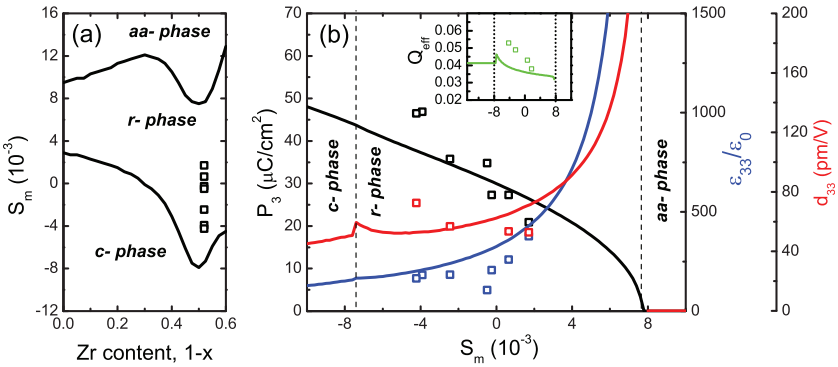

FIG. 3. (Color) (a) Calculated stability range of the *r*-phase in epitaxial PZT films as a function of Zr content (solid lines) and the obtained misfit strain values (open squares). (b) Calculated misfit strain dependence (solid lines) on P_3 (black), ε_{33} (blue) and d_{33} (red), and measured data points (open squares). The inset shows the calculated Q_{eff} (solid line) and obtained values (squares).

difference reflects the larger in-plane component of the polarization for higher S_M. The rotation angle between the polarization vector and the film plane is estimated as $\beta = \sin^{-1}(P_3/P_S)$. Here, we take P_S as an estimate for the length of the polarization vector. From Table I, it is seen that the polarization vector tends to rotate from the out-of-plane *c*-direction towards the *aa*-plane (low β) with increasing S_M.

The out-of-plane dielectric constant ε_{33} for all samples is determined as $\varepsilon_{33} = dP_3/(\varepsilon_0 dE_3)$ at $E = 0$. The obtained values (Fig. 3(b)) correspond well with theory as ε_{33} increases with higher strain values. It appears that P_3 and ε_{33} are approximately inversely related. From this point of view, roughly similar values for the effective piezoelectric response $d_{33,eff}$ can be expected, as they are dependent through the following equation:

$$d_{33,eff} \equiv \frac{\partial S_3}{\partial E_3} = \frac{\partial S_3}{\partial P_i}\frac{\partial P_i}{\partial E_3} = 2Q_{12,eff}(\varepsilon_0\varepsilon_{13}P_1 + \varepsilon_0\varepsilon_{23}P_2) + 2Q_{11,eff}\varepsilon_0\varepsilon_{33}P_3. \quad (1)$$

Here, $Q_{12,\mathrm{eff}}$, $Q_{11,\mathrm{eff}}$ ε_0, ε_{33}, and P_3 are the effective electrostrictive constants for a (001) oriented thin film strained symmetrically in plane, dielectric constant of vacuum, effective relative dielectric constant, and the spontaneous out-of-plane polarization, respectively.[4] Fig. 2(b) shows small signal effective d_{33} loops for samples S1, S5, and S7. In contrast to the *P-E* loops, the difference in d_{33}-*E* loops is not so pronounced. All parameters in Eq. (1) are field dependent; however, here we only consider the $d_{33,eff}$ at zero field. Note that these values can be significantly smaller than the maximum $d_{33,eff}$ observed for these samples (Table I).

Clamping causes the bulk, single crystal longitudinal electrostriction coefficient to be modified into an effective value Q_{eff}. For the (001) oriented epitaxial thin film, Q_{11} changes to $Q_{11,eff} = Q_{11} - (2s_{12}Q_{12})/(s_{11} + s_{12})$ and Q_{12} to $Q_{12,eff}$, where s_{ij} are the elastic compliances and Q_{ij} the electrostrictive coefficients for single crystal PZT.[4,11] For PZT thin films in the *c*-phase ($P_1 = P_2 = 0$), Eq. (1) reduces to $d_{33,eff} = 2Q_{11,eff}\varepsilon_0\varepsilon_{33}P_3$. Conventionally $d_{33,eff}$ is written as $d_{33,eff} = 2Q_{eff}\varepsilon_0\varepsilon_{33}P_3$. In the *r*-phase, Q_{eff} now also contains the contributions of the first two terms in Eq. (1), causing Q_{eff} to vary with strain; i.e., polarization rotation. In the inset of Fig. 3(b), the calculated Q_{eff} is shown together with the experimentally obtained values. It is noted that our method to obtain Q_{eff} is different from the one used by others, where ε_{33} was determined from *C-V* loops obtained at high frequency.[12] Our ε_{33} values are typically twice as low. Since the model only applies to data from static measurements, we choose to use the values from the quasi-static *P-E* loops. Overall, there is a good correspondence between the experimentally determined values and the model, considering that no fitting was applied.

The ferroelectric *r*-phase is a consequence of the monoclinic crystal structure and, therefore, different twin domains are expected. Such structural twin domains have been observed in monoclinic $BiFeO_3$ by XRD.[13] Yet, twins are not observed in our samples, and little experimental evidence for the monoclinic phase in PZT thin films is reported so far.[14] However, the properties of all our PZT films do fit well in Pertsev's predicted phase diagram, in which polarization rotation is only allowed in the monoclinic *r*-phase. The trends of the ferro and piezoelectric data evidence the existence of this monoclinic phase. Because of the limited TEC range of suitable substrates, it can be predicted that clamped (001) oriented epitaxial $Pb(Zr_{0.52}Ti_{0.48})O_3$ thin films under the same conditions will always end up in this phase.

In summary, we have epitaxially grown (001) oriented PZT thin film stacks using PLD. By changing the buffer-layers and/or substrates, thin films with different strain states have been obtained, caused by the TEC mismatch between PZT films and substrates. It is observed that P_3 and ε_{33} values in the PZT films are strongly dependent on this misfit strain. The piezoelectric coefficient $d_{33,eff}$, however, is hardly dependent on the substrate-induced strain, since P_3 and ε_{33} are approximately inversely related. We have shown that there is a good correspondence between measured data and theory. This supports the validity of the model for rotation of the polarization for clamped (001) oriented epitaxial $Pb(Zr_{0.52}Ti_{0.48})O_3$ thin films strained by the substrate and provides indirect experimental evidence for the monoclinic *r*-phase.

The authors gratefully acknowledge the support of the Smart Mix Programme of the Netherlands Ministry of Economic Affairs and the Netherlands Ministry of Education, Culture and Science, as well as the Vietnam's National Foundation for Science and Technology Development (NAFOSTED).

[1]K. J. Choi, M. Biegalski, Y. L. Li, A. Sharan, J. Schubert, R. Uecker, P. Reiche, Y. B. Chen, X. Q. Pan, V. Gopalan, *et al.*, Science **324**, 367 (2009).
[2]P.-E. Janolin, J. Mater. Sci. **44**, 5025 (2009).
[3]S. Gariglio, N. Stucki, J.-M. Triscone, and G. Triscone, Appl. Phys. Lett. **90**, 202905 (2007).
[4]N. A. Pertsev, V. G. Kukhar, H. Kohlstedt, and R. Waser, Phys. Rev. B. **67**, 054107 (2003).

[5]J. X. Zhang, D. G. Schlom, L. Q. Chen, and C. B. Eom, Appl. Phys. Lett. **95**, 122904 (2009).
[6]M. Dekkers, M. D. Nguyen, R. Steenwelle, P. M. te Riele, D. H. A. Blank, and G. Rijnders, Appl. Phys. Lett. **95**, 012902 (2009).
[7]For S2, 30 nm $SrTiO_3$ buffer-layer was deposited on Si by molecular beam evaporation; samples provided by D. G. Schlom, Cornell University, USA.
[8]P. Gerber, A. Roelofs, O. Lohse, C. Kugeler, S. Tiedke, U. Bottger, and R. Waser, Rev. Sci. Instrum., **74**, 2613 (2003).
[9]J. S. Speck and W. Pornpe, J. Appl. Phys. **76**, 466 (1994).
[10]For $SrTiO_3$, we find larger compressive strain than can be expected from TEC only. The additional strain could be attributed to the additional epitaxial strain.
[11]J. Haun, E. Furman, S.-J. Jang, and L. E. Cross, Ferroelectrics **99**, 45 (1989).
[12]A. L. Kholkin, E. K. Akdogan, A. Safari, P.-F. Chauvy, and N. Setter, J. Appl. Phys. **89**, 8066 (2001).
[13]H. W. Jang, S. H. Baek, D. Ortiz, C. M. Folkman, R. R. Das, Y. H. Chu, P. Shafer, J. X. Zhang, S. Choudhury, V. Vaithyanathan, *et al*., Phys. Rev. Lett. **101**, 107602 (2008).
[14]L. Yan, J. Li, H. Cao, and D. Viehland, Appl. Phys. Lett. **89**, 262905 (2006).